Flexural characterization of cell encapsulated PEGDA hydrogels with applications for tissue engineered heart valves

Christopher A. Durst, Michael P. Cuchiara, Elizabeth G. Mansfield, Jennifer L. West, K. Jane Grande-Allen *

Department of Bioengineering, Rice University, Houston, TX 77251-1892, USA

ARTICLE INFO

ABSTRACT

The limitations of the current clinical options for valve replacements have inspired the development of enabling technologies to create a tissue engineered heart valve (TEHV). Poly(ethylene glycol) diacrylate (PEGDA) hydrogel scaffolds permit greater biological and biomechanical customization than do non-woven mesh scaffold technologies. However, the material characterization of PEGDA hydrogels has been predominantly limited to compression and tension, as opposed to bending. Since large flexural deformations result in points of maximum stress in native valves as well as TEHVs, it is crucial to evaluate any potential scaffold material in this mode. The effect of formulation parameters on the bending mechanics of cell-seeded PEGDA hydrogels were investigated with a custom designed bending tester. Three molecular weights (3.4, 6, and 8 kDa) and three weight fractions (5%, 10%, and 15%, w/v) were subjected to three-point bending tests and the flexural stiffness was calculated. Manipulating the composition of the hydrogels resulted in flexural stiffnesses comparable with native tissues (15–220 kPa) with varied mesh sizes and swelling ratios. Hydrogels containing encapsulated valve cells, methacrylated heparin (Hep-MA), or both were substantially less stiff than acellular hydrogels. In conclusion, PEGDA hydrogels are an attractive potential scaffold system for TEHVs because they are not only cytocompatible and modifiable but can also withstand bending deformations. These studies are the first to explore the encapsulation of valvular interstitial cells in pure PEGDA hydrogels as well as to investigate the bending properties of PEGDA gels.

© 2011 Acta Materialia Inc. Published by Elsevier Ltd. All rights reserved.

1. Introduction

The near infinite biochemical and biomechanical tunability of hydrogels makes them very attractive potential scaffold materials for tissue engineered heart valves (TEHVs). Hydrogels have received far less attention than other scaffolding materials, with the majority of TEHV investigations being performed using non-woven fiber mesh or salt-leached foam scaffolds generated from polyglycolic acid, poly(lactic acid–co-glycolic acid), and polyhydroxyalkanoates [1–5]. Thus far, these materials have been used as scaffolds for the most successful TEHV to date (in both in vitro and in vivo evaluations) [6]. Their open structure allows cell migration throughout the scaffold, and their material properties can be engineered to be sufficient for the mechanical environment of the valve, which involves flexure, tension, compression, and shear varying throughout the cardiac cycle. Additionally, these materials are degradable and have been FDA approved for many years. However, these materials have shown certain limitations, namely their high initial stiffnesses compared with native tissues and the substantial length of time required for the polymer to undergo hydrolysis-governed degradation [7]. Furthermore, these materials lack intrinsic biological functionalization, meaning that they do not present any functional biological moieties that could direct cell signaling, ECM production, or enzyme-governed degradation. These materials can be modified to present these motifs, however, there is no control over functional molecule localization (in contrast to the patterned localization achievable in hydrogels via photolithographic or two-photon adsorption methods) [8–10].

Both non-woven fiber mesh and salt-leached foam scaffolds use cytotoxic processing conditions to generate their architecture. Since the polymer processing conditions are cytotoxic, cell seeding must be performed after the scaffold is fabricated. Cell seeding has been one of the most significant challenges in the use of these scaffold materials. Seeding methods have resulted in inhomogeneous cell distributions, low densities, and long seeding times before the scaffolds were populated. Initially, cells were incubated on the scaffolds under static conditions for up to 4 days in order to allow cell migration to the interior of the scaffold [11]. Dynamic seeding methods were developed that yielded homogeneous and slightly more efficient seeding, but the dynamic nature of the

* Corresponding author.
  E-mail address: grande@rice.edu (K.J. Grande-Allen).

seeding environment was reported to cause small cracks in the scaffold material [12]. Encapsulation has been shown to be the most efficient and homogeneous method of cell seeding. For example, the use of a viscous fibrin "cell carrier" gel resulted in fast, high yield, homogeneous seeding of valvular interstitial cells (VICs) into fiber matrices. The use of fibrin as the basis for the gel, however, alters the local biochemical environment of the cell through both its structure (cell substrate) as well as the retention of bioactive molecules within the gel [13,14]. While these previous approaches hold promise, we believe that the ability to encapsulate cells coupled with the customization potential of polymeric biomaterials makes hydrogels very appealing as scaffold systems.

Poly(ethylene glycol) diacrylate (PEGDA) hydrogels are intrinsically biocompatible, since the base (unmodified) gels are biologically neutral, resist protein adsorption, do not release acidic products during their degradation and can be crosslinked with low cytotoxicity, allowing for high density three-dimensional (3-D) cell encapsulation. Furthermore, poly(ethylene glycol) (PEG) hydrogels can be modified by crosslinking a large number of bioactive moieties (peptides, glycosaminoglycans, growth factors) to achieve a high degree of specific bioactivity [15–17]. Indeed it is widely reported that peptides tethered to either the surface or bulk phase of PEGDA gels will retain their bioactivity after this modification [18–20]. Additionally, since these materials can be rapidly photopolymerized, spatial control of functional moieties is possible both two-dimensionally and three-dimensionally, due to the emerging field of two-photon stereolithographic fabrication techniques [9].

The physical properties of PEGDA gels can be modified across a continuum of magnitudes that are biologically relevant in terms of recapitulating both tissue function and the pericellular environment. Hydrogel physical properties such as stiffness, degree of swelling, and effective diffusivity can be controlled by manipulating the molecular weight of the macromer, the weight fraction of macromer in solution and the crosslinking time [21,22]. Stiffness was of primary interest in this paper, and the construct stiffness achieved ranged from very low ($\sim$5 kPa, similar to a 1% HA gel [23], which could mimic the gelatinous spongiosa [24]), to several orders of magnitude higher (400 kPa, similar to bovine pericardium [25]). It has been further demonstrated that crosslinking density affects the strain experienced by the cell, and certain formulation parameters can translate nearly 100% of bulk strain to individual cells [26]. Cells seeded in fiber mesh scaffolds can be in contact with either a single fiber or many fibers, which may have varying degrees of displacement at the microstructural level due to macrostructural strain. Thus, mechanotransduction in hydrogels appears to be more efficient than in fiber meshes.

While polymer hydrogels have been well studied in tension and compression, the flexural properties of these gels have yet to be investigated. Since flexure represents a major mode of deformation of heart valve leaflets, the purpose of this study was to investigate the behavior of these gels in three-point bending. We hypothesized that cell encapsulated PEGDA gels could be formulated to approximate the flexural stiffness of fresh porcine aortic valve leaflets, and that these gels would support short-term maintenance of the VIC phenotype and extracellular matrix (ECM) synthesis. This exploration of PEGDA gels with respect to their capacity to achieve the mechanical requirements of engineered heart valve leaflets will aid in the translation of hydrogels to more biomimetic scaffold fabrication and realistic in vitro testing of hydrogel-based TEHVs.

2. Materials and methods

All chemicals were purchased from Sigma (St. Louis, MO) unless otherwise noted.

2.1. Study design

The primary concern of this study was to investigate the effect of hydrogel formulation parameters on the flexure properties of TEHV scaffolds. As a result, the experiment employed a full factorial design for the flexural testing and immunofluorescence studies of cell-seeded gels, and flexural, compression, and network property characterization of acellular gels (Fig. 1A). Sample sizes were chosen based on prospective statistical power calculations. Using two-way ANOVA comparison of the row $\times$ column means, where the detectable contrast was chosen to be 0.4, the standard deviation was set at 0.15 (on the upper bound of what has been reported in hydrogel compression testing [26,27]), and n = 5, the statistical power was determined to be 0.8. As the study was underway it became evident that heparin altered the gel properties in an unexpected way, and subgroups were added to attempt to address the effect of heparin incorporation on gel mechanical properties (Fig. 1B). These subgroups were tested using lower sample sizes than the samples used in the primary focus of the paper.

2.2. Cell culture

Primary cultures of VICs were isolated from aortic valve leaflets from 6-month-old pigs obtained from a local abattoir (Fisher Ham and Meat, Spring, TX) within 6 h of slaughter. The valve leaflets were dissected using sterile techniques and rinsed with sterile phosphate-buffered saline (PBS) supplemented with 5% antibiotic–antimycotic solution (ABAM, Cellgro, Manassas, VA). The leaflets were then placed in a flask containing serum-free Dulbecco's modified Eagle's medium (DMEM) (Cellgro) supplemented with 2 mg ml^{-1} collagenase type II (Worthington, Lakewood, NJ) and 2.5% ABAM. The flask was incubated at 37 °C in an incubated shaker for 30 min. Next, the leaflets were removed from solution and the endothelial cells were removed by rubbing the surface of the valve with a cotton swab. The leaflets were then minced using a No. 10 scalpel and digested using 2 mg ml^{-1} collagenase type III, 0.1 mg ml^{-1} testicular hyaluronidase (Worthington), 2 mg ml^{-1} protease, 2.5 vol.% HEPES, and 2.5 vol.% ABAM in serum-free DMEM for 4 h in an incubated shaker (150 rpm). The cell suspension was filtered using a 70 μm pore size cell strainer (BD Falcon, Franklin Lakes, NJ), pelleted, and cultured on tissue culture polystyrene in DMEM supplemented with 10% bovine growth serum (BGS, Hyclone, Logan, UT) and 1% ABAM. VICs were maintained in a humidified incubator at 37 °C with 5% CO$_2$. Medium was changed every 2 days. All experiments were performed using cells between passages 4 and 8.

2.3. PEGDA synthesis

PEGDA was prepared using previously described methods [17]. Briefly, 0.1 mM dry poly(ethylene glycol) with a molecular weight of either 3.4, 6, or 8 kDa was combined with 0.4 mM acryloyl chloride and 0.2 mM triethyl amine in anhydrous dichloromethane. The reaction was stirred overnight under argon at 22 °C. The solution was washed with 2 M K$_2$CO$_3$ in order to remove HCl. Gravity-based phase separation was used to separate the solution into an aqueous and organic phase. The organic (PEGDA-containing) phase was removed the next day and dried with anhydrous MgSO$_4$. PEGDA was then precipitated with cold diethyl ether, filtered, and dried under vacuum. ^{1}H NMR was used to verify acrylation of the PEG chains by the presence of peaks at 3 ppm. MALDI-TOF was used to verify the molecular weight of the synthesized PEGDA. PEGDA was stored at -20 °C under argon until use.
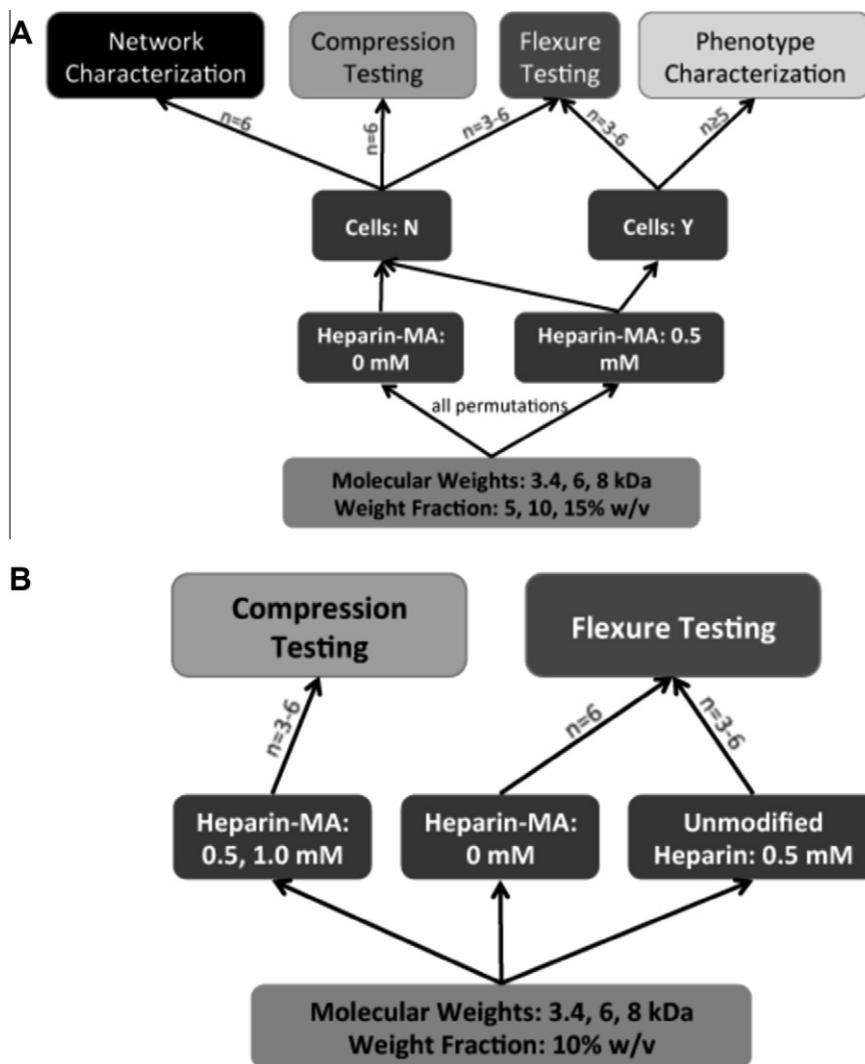
Fig. 1. (A) Diagram of the experimental design. A full factorial design was chosen to investigate the effect of varying formulation parameters (molecular weight, weight fraction) on cell phenotype and hydrogel network and mechanical properties. Sample sizes were chosen from prospective power calculations. (B) Diagram showing sub-studies investigating the effect of heparin inclusion on the gels.

2.4. Methacrylation of heparin

Heparin was methacrylated using previously described methods for the methacrylation of polysaccharides [15,28]. In short, the procedure involved dissolving heparin in ddH$_2$O at 2% (w/v), reacting the solution with a 20 times molar excess of methacrylic anhydride, and adjusting the pH to 7.5 using 4 N NaOH. This solution was stirred on ice for 24 h. while maintaining pH at 7.5. The methacrylated heparin (Hep-MA) was precipitated from solution with 4 °C ethanol, then dialyzed for 48 h using a 1000 Da molecular weight cut-off filter (Spectrum Laboratories, Rancho Dominguez, CA). The solution was then dialyzed and the powder was stored under argon at −20 °C until use. ^{1}H NMR was used to determine methacrylation per disaccharide repeat unit.

2.5. Hydrogel polymerization

In order to test the effects of a wide range of hydrogel formulation parameters on bending mechanics a full factorial design was employed. Because the molecular weight and weight fraction of the macromer are known to affect the material behavior of the resulting hydrogels [21], three different molecular weights (3.4, 6, or 8 kDa) and three weight fractions (5%, 10%, or 15%, w/v) were

investigated in a combinatorial study (nine permutations). For each permutation a specific molecular weight of PEGDA was dissolved in PBS to a specific weight fraction, after which Hep-MA was added to obtain a final concentration of 0.5 mM Hep-MA in the prepolymer solution. The photoinitiator 2-hydroxy-4′-(2-hydroxyethoxy)-2-methylpropiophenone was dissolved in ethanol at 10% (w/v) and added to the prepolymer solution at 3 vol.%. The resulting solution was sterile filtered and VICs were added to the solution at a concentration of 22×10^6 cells ml^{-1}.

Prior to polymerization the prepolymer solution was poured into custom molds. The molds were created from glass slides separated by comb-shaped polycarbonate spacers, resulting in seven $6 \times 44 \times 0.8$ mm (width × height × thickness) wells per mold assembly. Prior to molding the glass slides and polycarbonate spacers were coated with Sigmacote (Sigma–Aldrich, St. Louis, MO) to ease removal of the crosslinked hydrogels from the molds. The molds were steam sterilized, assembled, and, after cooling, the prepolymer was loaded into the molds. Subsequently the gels were crosslinked with longwave UV light (365 nm, 10 W cm^{-2}) for 10 min. The hydrogels were removed from the molds and cultured separately in 6-well plates (BD Falcon, BD Bio Sciences, San Jose, CA) for 48 h in a humidified incubator before mechanical testing.

To determine the impact of cell inclusions on hydrogel bending behavior, acellular gels were created in the same manner as above for all nine permutations of molecular weight and weight fraction. In order to elucidate the effect of Hep-MA subsets of hydrogel formulations were created in the same manner as above, except that either (i) the heparin used was not methacrylated (10% weight fraction for all molecular weights plus 15% for 8 kDa) or (ii) the concentration of Hep-MA was varied (10% weight fraction for all molecular weights). An additional control set of "base" PEGDA hydrogels (all nine permutations of molecular weight and weight fraction) was prepared without any Hep-MA.

2.6. Mechanical testing

The hydrogel strips were loaded into a custom built bending tester (design adapted from Gloeckner et al. [29]) and subjected to three-point bending tests. To permit optical tracking of hydrogel deformation, small graphite particles were sifted over the test strip, the reference rod, and a calibrated flexure bar (Fig. 2) [7]. A stepper motor was coupled to a micropositioner in order to achieve linear motion of the loading posts. This apparatus was used to deform the sample by pulling the center of the sample against a flexure bar at a strain rate of 1.5 mm min^{-1} until a maximum change in curvature (ΔK) of 0.3 mm^{-1} was achieved. Images of the sample deformation and graphite particle movement were captured at 5 frames per second by a CCD camera (Leica DFC320) mounted over the apparatus. The deformation of the sample was determined from the images by custom Matlab scripts, which calculated the least squares regression of these points to a quadratic line. Using derivatives of this line the curvature of the sample was calculated using Eq. (1):

$$k = \frac{y''}{(1 + (y')^2)^{3/2}} \qquad (1)$$

where y is the quadratic fit through the points on the sample.

The deflection of the calibrated flexure bar was also determined from each image and used to calculate the force applied to bend the sample. From the load data the moment was calculated and applied in the Bernoulli–Euler beam bending equation (Eq. (2)) to determine bending stiffness:

$$M = E_{\text{eff}} I \Delta K$$

where

$$I = \frac{1}{12} t^3 h$$

Rearrange for modulus

$$E_{\text{eff}} = 12 \frac{M\Delta K}{t^3 h} \qquad (2)$$

where E_{eff} is the flexural stiffness, I is the second moment of area, ΔK is the curvature (from Eq. (1)), t the is sample thickness, and h is the sample height. A sample moment–curvature plot can be seen in the Supplemental information (Supplemental Fig. 1).

Sample size for all flexure groups was $n = 3–6$ per hydrogel permutation. After flexure testing the cellularized gels were retained for immunocytochemical staining.

In order to verify the stiffness results obtained from bending, several additional sets of PEGDA hydrogels were tested in compression. PEGDA slabs with an initial thickness of 3 mm were created (as in Section 2.4, with the exception of using 3 mm spacers), punched with a 3 mm biopsy punch, swollen in medium, and compressed. The gels were compressed to 50% strain at 0.1 mm s^{-1} between stainless steel platens in a Bose-Enduratec ELF3200 (Bose Electroforce, Eden Prairie, MN). After converting load–displacement data to stress–strain data, stiffness was measured
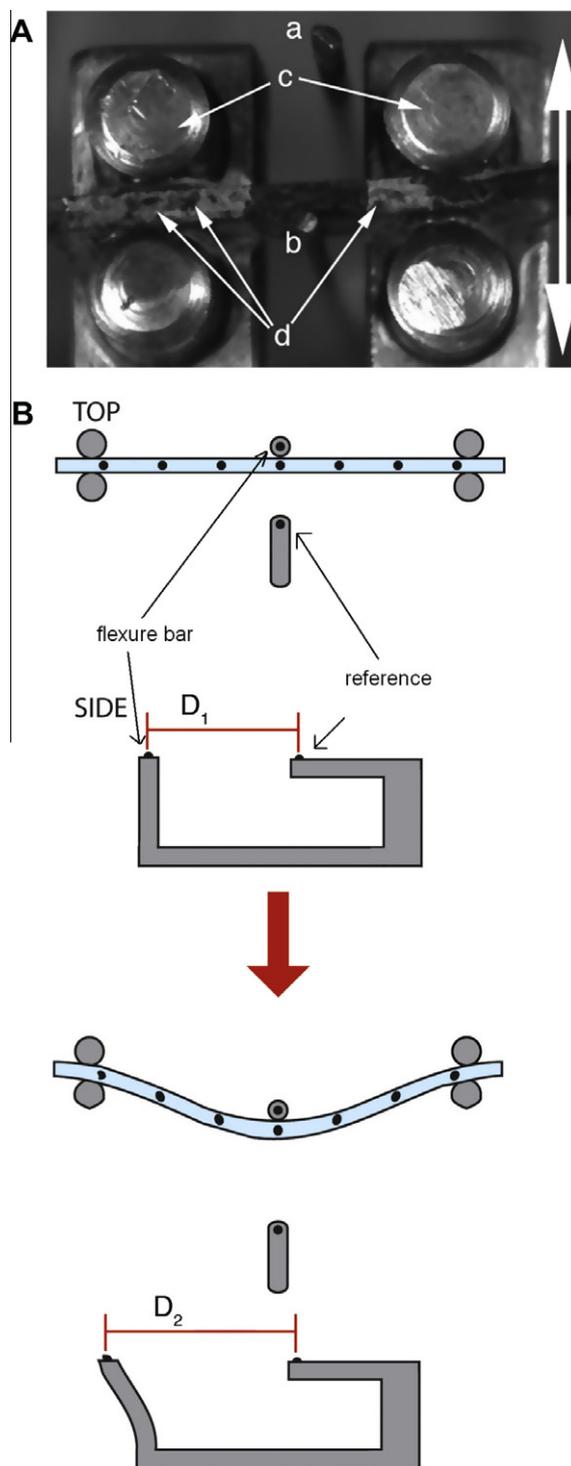
Fig. 2. (A) Photograph with annotations depicting the method of operation of the bending apparatus. The linear motion of the bending tester stage pulls the hydrogel strip (secured against the loading posts (c)) against the flexure bar (b). Displacement of the flexure bar is determined relative to the immobile reference bar (a). Graphite particles (d) are visible atop the hydrogel strip. The arrow indicates the direction of motion. (B) Illustration demonstrating the concept behind optical strain measurement in the three-point bending test. This method was originally described by Gloeckner et al. [29].

from the linear portion of the stress–strain curve at 15–30% strain. Compression testing was also performed to determine whether there was an influence of Hep-MA concentration (0.5 or 1.0 mM) on hydrogel stiffness. All compressive testing groups had a sample size of $n = 5–6$ for each hydrogel formulation.

2.7. Cellular analyses

To assess the viability of the VICs following encapsulation, freshly prepared cell-seeded hydrogels were stained with a Live/Dead kit (Molecular Probes, Carlsbad, CA). After staining for 30 min the hydrogels were imaged using a Zeiss LSM 510 confocal microscope (Carl Zeiss Microimaging, Thornwood, NY) to assess the abundance and location of live cells (green calcien AM) or dead cells (red ethidium homodimer-1).

To assess the VIC phenotype and capacity for collagen synthesis the gels were cultured for 2 days in static culture (using the same medium and culture conditions as for two-dimensional (2-D) culture explained in Section 2.1) and then stained with rabbit anti-smooth muscle α-actin (αSMA) (Abcam, Cambridge, MA) and mouse anti-prolyl-4-hydroxylase (P4H) (Chemicon, Billerica, MA) [15,30]. Primary antibodies were used at 1:100 dilution in 0.1% (w/v) bovine serum albumin (BSA) in PBS and allowed to diffuse into the hydrogel for 16 h at 4 °C on a rocker table at room temperature. Gels were then washed with 0.1% BSA in PBS for 4 h on a rocker table. After washing the gels were incubated simultaneously with fluorescently tagged secondary antibodies (AF-488 conjugated donkey anti-mouse, AF-633 conjugated goat anti-rabbit, Molecular Probes, Carlsbad, CA) for 16 h at 4 °C on a rocker table. Secondary antibodies were used at 1:1000 dilution in 0.1% BSA in PBS. Finally, the gels were washed with 0.1% BSA in PBS for 4 h on a rocker table and subsequently imaged.

The proportions of αSMA- and P4H-positive cells were determined in order to assess maintenance of the myofibroblast phenotype. First, the channels in the confocal images were separated in ImageJ. Next, the background was subtracted using a rolling ball method with a radius of 25 pixels. The images were extracted using threshold values above the background intensity obtained from secondary antibody only controls. Lastly, a particle analysis algorithm was used to count cells with a particle size greater than 5 μm^2 and circularity in the range 0.5–1.0. The total counts for αSMA- and P4H-positive cells were normalized to the total cell count (4′,6-diamidino-2-phenylindole (DAPI) staining) in each frame and at least five images were used for each group.

2.8. Hydrogel network characterization

The hydrogel network was characterized using Flory–Rehner theory. The wet mass of the gels was measured after cellular analyses and mechanical testing. After the gels had been lyophilized for 48 h their dry mass was measured. From this information and the formulation parameters the mesh size (Eq. (3)), swelling information, and molecular weight between crosslinks (Eq. (4)) were calculated as previously described by Cruise et al. [31].

$$\xi = (r_0^{-2})^{1/2} V_{2,s}^{-1/3} \quad (3)$$

where r_0 is the average end-to-end distance of the polymer, and $V_{2,s}$ is the polymer volume fraction in the swollen state.

$$M_c = (V_e + \frac{2}{M_{n(0)}})^{-1} \quad (4)$$

where V_e is the number of effective chains per unit volume and M_n is the number average molecular weight of the starting polymer.

2.9. Statistical analysis

Statistical analyses of stiffnesses and network parameters were performed using JMP (SAS Software, Cary, NC). Where appropriate, either one- or two-factor ANOVA was performed and fitted to a least squares model. Subgroup means were compared by post hoc Tukey's HSD test at $\alpha = 0.05$. When represented visually the

data are expressed as means ± standard errors. Letters are used to denote significance in the figures (groups are significantly different if they do not have a letter in common).

3. Results

3.1. Characterization and verification of the polymer products

The molecular weight of the synthesized PEGDA was verified by mass spectrometry to be within 150 Da of the specified molecular weight of the precursor (PEG) for all molecular weights of PEG. The polydispersity indices were calculated to be 1.053, 1.007, and 1.0574 for 3.4, 6, and 8 kDa PEGDA, respectively. Acrylation efficiency was verified by the presence of peaks at 3 ppm in NMR spectra for all PEGDA samples. Percent methacrylation for heparin was 3.7%.

3.2. Hydrogel material properties

As expected, decreasing the molecular weight of the PEGDA in unmodified, acellular hydrogels (containing no Hep-MA) resulted in stiffer gels in flexure (Fig. 3A). For equivalent weight fractions
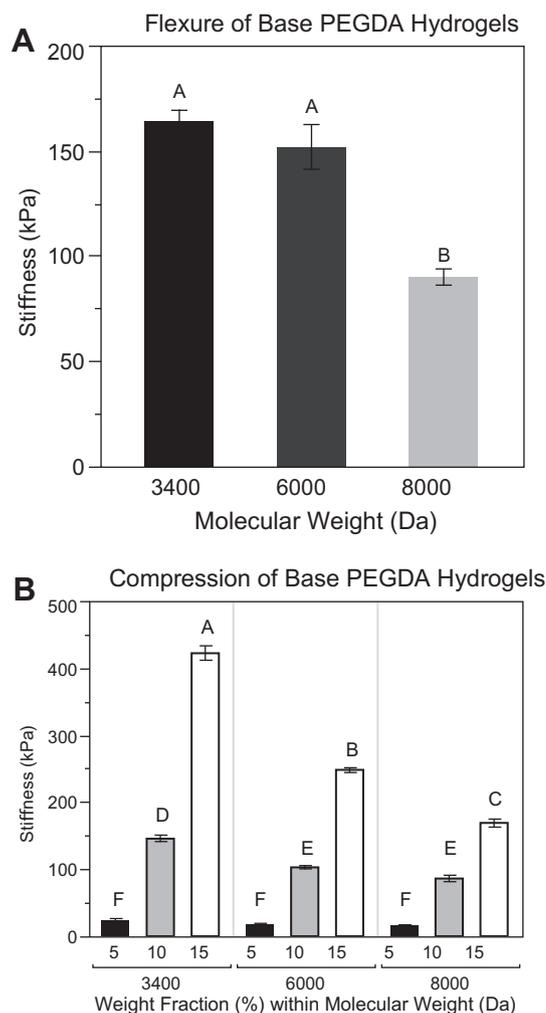
Fig. 3. (A) Flexural stiffness of base PEGDA hydrogels (unmodified, containing no Hep-MA). Hydrogels were all 10% PEGDA by weight. (B) Compressive stiffness of the base PEGDA hydrogels. Flexural stiffnesses are of the same order of magnitude as compressive stiffnesses for the 10% weight fraction hydrogels. Samples that do not share a common letter are significantly different at $\alpha = 0.05$. $n = 6$ for all sample groups.

gels in compression (Fig. 3B) showed similar moduli to gels in flexure, so it was concluded that the stiffnesses measured by the flexure device were valid. Compressive stiffness of the unmodified, acellular hydrogels was observed to increase with increasing weight fraction and to decrease with increasing molecular weight.

Since heparin is a charged molecule, inclusion of heparin was expected to alter the swelling properties of the gel, although it is unknown what impact there would be on the material properties. In acellular gels containing 0.5 mM Hep-MA (Fig. 4A) stiffness again increased significantly with increasing weight fraction for each molecular weight ($P < 0.05$). Interestingly, there was either no change in stiffness or a trend of increasing stiffness with increasing molecular weight, which was the opposite of what was expected given the data from testing unmodified PEGDA hydrogels (Fig. 4B). To evaluate whether this deviation from the expected pattern was due to the methacrylation of heparin, PEGDA hydrogels containing unmodified heparin (0.5 mM) were tested in flexure (Fig. 4B). Although there was no difference in flexural stiffness between hydrogels modified with entangled unmodified heparin and Hep-MA for the lower molecular weights of PEG, the stiffness of the 8 kDa PEGDA hydrogels was significantly lower for the unmodified heparin case at PEGDA weight fractions of both 10% (Fig. 4B, $P < 0.01$) and 15% (70 kPa for unmodified heparin vs. 209.7 kPa for Hep-MA, results not shown, $P < 0.01$). To determine whether Hep-MA interfered with stiffness in a concentration-dependent manner, hydrogels containing either 0.5 or 1.0 mM Hep-MA were tested in compression. The 3.4 kDa PEGDA hydrogels with the greater Hep-MA concentration were less stiff (Fig. 4C), but there was no significant effect of Hep-MA concentration at the higher molecular weights of PEGDA. It is also noteworthy that for those hydrogels tested in compression the inverse relationship between stiffness and molecular weight was again present, i.e. the addition of heparin to PEGDA hydrogels affected the flexural characteristics more than the compressive behavior.
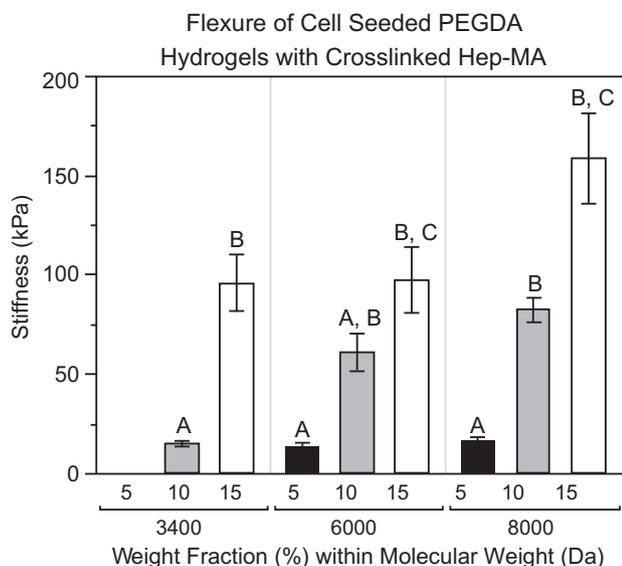
Finally, cell-seeded PEGDA gels with 0.5 mM Hep-MA were tested in flexure (Fig. 5). These samples demonstrated trends that were very similar to the flexural stiffnesses of acellular hydrogels containing Hep-MA (Fig. 4A). For each molecular weight the stiffness increased with increasing weight fraction ($P < 0.05$). Additionally, stiffness was either unaffected or generally increased with increasing molecular weight, in contrast to the patterns shown in Figs. 3B and 4C. It is also evident that the inclusion of cells reduced the hydrogel stiffness for all formulations compared with acellular gels ($P < 0.05$).

3.3. Network properties of acellular hydrogels

The network properties of the gel were investigated to verify the observed mechanical phenomena and to ensure that the diffusional properties were sufficient for cell viability and immunostaining. For hydrogels prepared without heparin the molecular weight between crosslinks decreased with increasing weight fraction and increased with increasing molecular weight, as expected (Table 1, Supplemental Fig. 2). Adding Hep-MA to these gels resulted in a similar pattern at 3.4 and 6 kDa, however, this trend was lost at the highest molecular weight (8 kDa). Decreasing the molecular weight between crosslinks typically results in a stiffer gel, so these results were consistent with the material behavior of the unmodified (base) hydrogels (Table 1, Supplemental Fig. 2). For the hydrogels containing Hep-MA this relationship between molecular weight between crosslinks and stiffness was only evident for the lowest molecular weight PEGDA hydrogels (3.4 kDa). As shown in Table 1 and Supplemental Fig. 3, mesh sizes
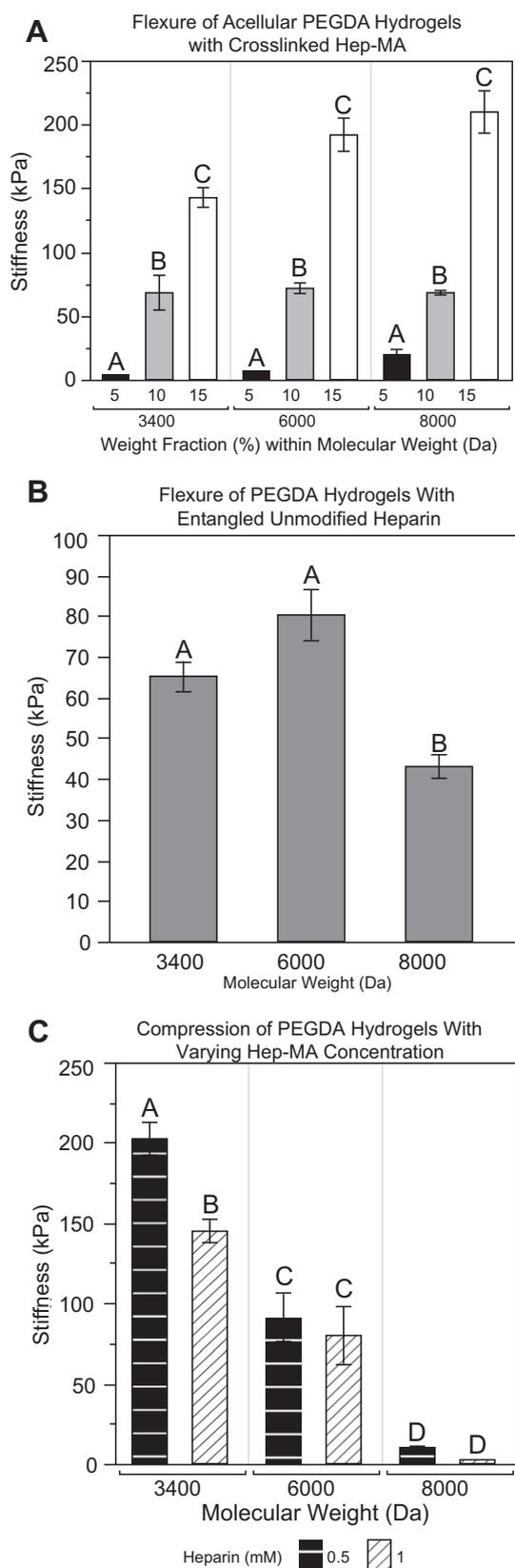
Fig. 4. (A) Flexural stiffness of acellular gels containing 0.5 mM Hep-MA. (B) Flexural stiffness of representative groups of PEGDA hydrogels containing 0.5 mM unmodified heparin. (C) Compressive stiffness of PEGDA discs containing Hep-MA at concentrations of either 0.5 or 1.0 mM. $n = 3$–6 for all groups. Samples that do not share a common letter are significantly different at $\alpha = 0.05$.

Fig. 5. Flexural stiffness of cell-seeded gels. n = 3–6 for all samples. Samples that do not share a common letter are significantly different at α = 0.05.

Table 2
Percentage of cells expressing smooth muscle α-actin (top) and prolyl-4-hydroxylase (bottom) for each composition of gel.
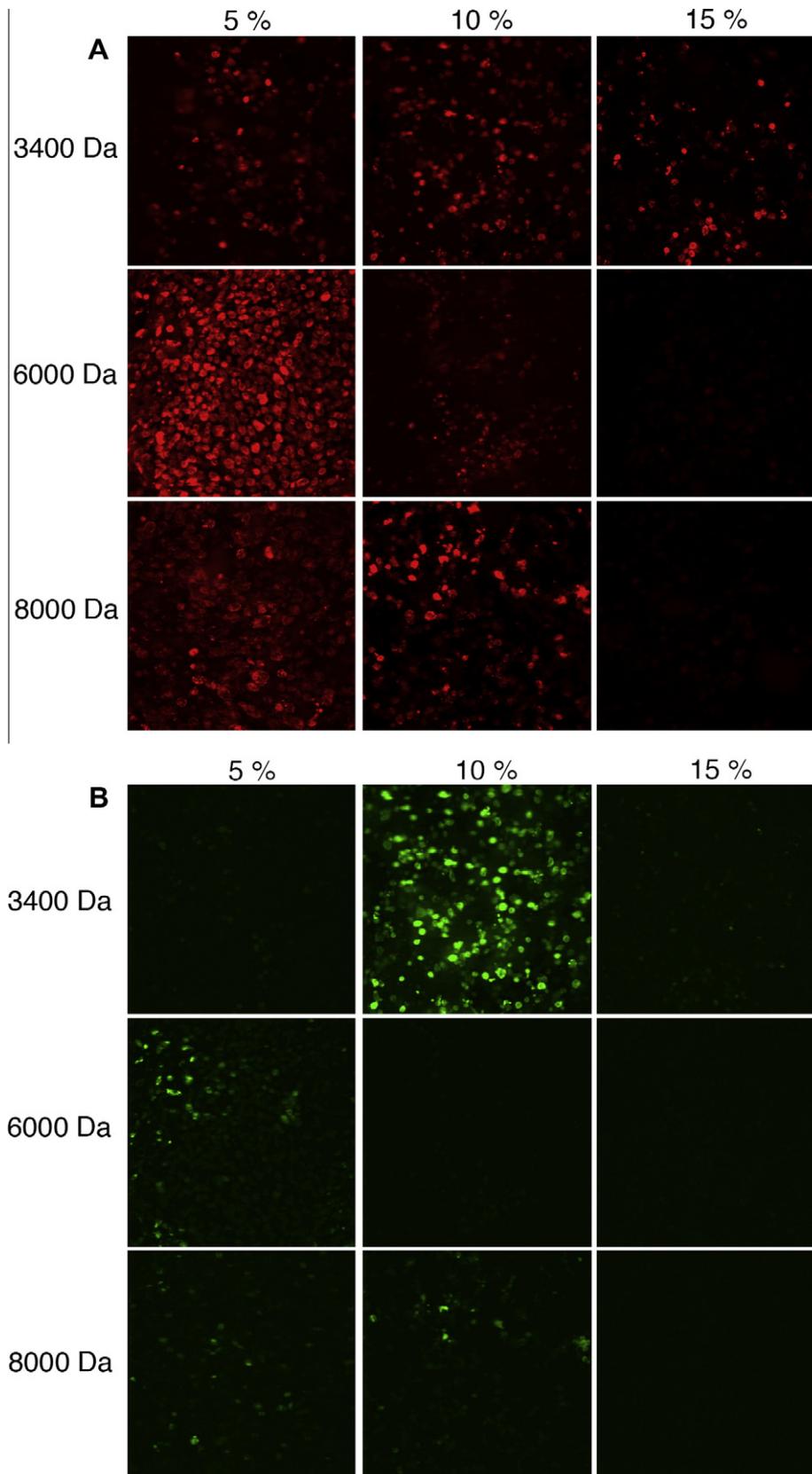
Molecular weight (Da)	Weight fraction (%)	Percentage of cells expressing marker ± standard error	
		αSMA	P4H
3400	5	0.68 ± 0.06	0.01 ± 0.02
	10	0.70 ± 0.06	0.14 ± 0.02
	15	0.71 ± 0.05	0.02 ± 0.01
6000	5	0.90 ± 0.05	0.06 ± 0.01
	10	0.47 ± 0.06	0.00 ± 0.02
	15	0.72 ± 0.05	0.03 ± 0.01
8000	5	0.56 ± 0.06	0.02 ± 0.01
	10	0.12 ± 0.06	0.00 ± 0.02
	15	0.11 ± 0.06	0.00 ± 0.02

$n \geqslant 5$ For all samples.

(Table 2). This was maintained in the 15%, 3.4 kDa gel, but lost in the 15%, 6 kDa and 15%, 8 kDa gels. P4H-positive cells were sparse in all gels, and were not seen at all in the 15%, 6 kDa and 15%, 8 kDa gels (Fig. 6).

4. Discussion

Hydrogels are rapidly garnering interest within the valve community as potential scaffolds for TEHVs, but further investigation is needed about the ability of hydrogels to support the culture of VICs and about their material behavior, particularly in flexure. In contrast to the large body of information about TEHVs generated using polymer meshes or foams, the study of VIC encapsulation within hydrogels is in the nascent stage, with only three studies currently published, albeit with some differences to the hydrogel materials presented in this paper [14,32,33]. The function of VICs encapsulated in PEG hydrogels was investigated in a recent paper by Benton et al. [34]. Although previous work has focused on the important characteristics of cell phenotype and function, it is just as relevant to examine material properties, due to both the mechanical demands of the in vivo environment as well as the impact of pericellular substrate stiffness on cell function. Furthermore, since flexure constitutes a major mode of deformation for heart valves, and it is reported that maximum sites of stress are

in the base and heparinized hydrogels demonstrated the same data patterns, or lack thereof, as found for molecular weight between crosslinks. Swelling ratios for the various hydrogel formulations increased slightly with PEG molecular weight, but this effect was much less pronounced than for the other network properties (Table 1, Supplemental Fig. 4). Swelling ratios decreased with increasing weight fraction of PEGDA. Finally, the overall magnitudes of mesh size and swelling ratio were lower for the heparinized hydrogels compared with the base hydrogels. However, molecular weight between crosslinks was only significantly lower in the heparinized gels than the base gels within at the 6 kDa, 5% and 8 kDa, 5% formulations.

3.4. Cell phenotype assessment

In gels with weight fractions of 5% and 10% (irrespective of molecular weight) the majority of cells were positive for αSMA

Table 1
Calculated network properties for acellular hydrogels.

Group	Molecular weight (Da)	Weight fraction (%)	Molecular weight between crosslinks (Da)	Mesh size (Å)	Mass swelling ratio (Q)
Heparinized		5	859.73 ± 118.89	99.42 ± 10.52	19 ± 1.96
	3400	10	647.03 ± 63.29	71.11 ± 5.06	10.56 ± 0.61
		15	481.77 ± 22.06	54.54 ± 1.68	7.34 ± 0.17
		5	1461.13 ± 93.54	137.52 ± 6.76	22.32 ± 1.13
	6000	10	1103.05 ± 154.46	99.58 ± 10.22	13.11 ± 1.32
		15	1054.92 ± 32.86	90.64 ± 2.02	10.39 ± 0.21
		5	1140.73 ± 153.82	111.8 ± 10.56	17.71 ± 1.25
	8000	10	1324.46 ± 202.6	110.29 ± 12.54	13.68 ± 1.32
		15	898.89 ± 142.44	79.4 ± 8.8	9.03 ± 0.75
Non-heparinized		5	1065.56 ± 50.6	117.83 ± 5.02	22.53 ± 1.29
	3400	10	677.23 ± 10.83	73.61 ± 0.84	10.81 ± 0.11
		15	546.42 ± 4.2	59.43 ± 0.31	7.85 ± 0.03
		5	1471.94 ± 45.61	138.2 ± 3.32	22.35 ± 0.58
	6000	10	1143.68 ± 17.69	102.17 ± 1.14	13.18 ± 0.14
		15	941.97 ± 20.85	83.68 ± 1.3	9.69 ± 0.13
		5	2051.76 ± 121	172.35 ± 8.15	26.41 ± 1.4
	8000	10	1505.62 ± 78.13	121.7 ± 4.61	14.78 ± 0.55
		15	1421.79	109.84 ± 2.75	11.82 ± 0.27

The table lists means ± SEM for molecular weight between crosslinks, mesh sizes, and mass swelling ratios for acellular gels with 0 and 0.5 mM Hep-MA. Molecular weight between crosslinks decreases with increasing weight fraction in both heparinized and non-heparinized gels. In non-heparinized gels the molecular weight between crosslinks increases with increasing molecular weight. In heparinized gels this trend is observed from 3.4 to 6 kDa, but is not seen at higher molecular weights. Mesh size decreases with increasing weight fraction in both heparinized and non-heparinized gels. In non-heparinized gels mesh size increases with increasing molecular weight. Samples marked with different letters are significantly different at α = 0.05.

Fig. 6. Representative immunostaining of (A) smooth muscle α-actin and (B) prolyl-4-hydroxylase in cell-encapsulated hydrogels for each composition of hydrogel.

due to flexure in the in vivo environment [35], it is prudent that any potential TEHV scaffold undergoes flexural characterization in vitro. It has been reported that the incorporation of heparin into hydrogels is necessary to maintain the normal phenotype of VICs (in 2-D culture), however, recently published data have demonstrated methods to preserve the VIC phenotype by careful choice

of the gel formulation [15,34]. This data was the motivation for the use of Hep-MA in this manuscript. By methacrylating heparin it can be covalently bonded to the hydrogel bulk and its bioactivity could be retained. The tests performed in this study demonstrated that functionalizing the gels with immobilized heparin caused flexural stiffness to decrease. However, the resulting range of flexural moduli (up to 400 kPa), even in the hydrogels containing Hep-MA (up to 200 kPa) and encapsulated cells (up to 160 kPa), while lower than that of native tissue (703.05 kPa against curvature, 491.69 kPa with curvature [36]; we performed three-point bending on a limited number of aortic valve leaflets with our tester and obtained results of the same order of magnitude), was of the same order of magnitude of both bovine pericardium (400 kPa cross fiber [25], commonly used in bioprosthetic valves) and virgin polyglycolic acid/poly-L-lactic acid meshes (∼250 kPa [2], commonly used for valvular tissue engineering).

The network properties, which were calculated to further characterize these hydrogels, suggested that the incorporation of Hep-MA disrupted network formation by the crosslinked PEGDA. For example, it was expected that lower values for molecular weight between crosslinks would correspond with stiffer gels. Indeed, when considering each hydrogel class (i.e. heparinized) separately, molecular weight between crosslinks followed the expected trends of decreasing with increasing weight fraction and increasing with increasing molecular weight. When comparing gels with and without heparin the incorporation of heparin did not statistically have an impact on the molecular weight between crosslinks of the resulting gels (with the exception of 6 kDa, 5% and 8 kDa, 5%). This result indicates that there are additional phenomena that govern gel stiffness when heparin is immobilized within the network. One potential explanation is that the negative charge or size of the heparin molecule could be interfering with network formation, thus inhibiting complete crosslinking of the PEGDA gel. This explanation was tested by varying the concentration of Hep-MA in gels in compression and it was confirmed that gels containing 1.0 mM Hep-MA were less stiff than gels containing 0.5 mM Hep-MA (Fig. 4C). To investigate whether this was a size-dependent phenomenon gels were doped with unmodified heparin. Gels doped with 0.5 mM heparin were less stiff than gels functionalized with the same concentration of Hep-MA, suggesting that the potential multiple crosslinking sites per heparin molecule increase stiffness and that chain entanglement is not the only means of retaining the heparin molecule. Collectively, these studies indicate that the negative charge of the heparin molecule is likely inhibiting the formation of radical polymerization sites and that incomplete crosslinking is obtained when either heparin or Hep-MA is included. This inhibition of complete crosslinking, however, appears to be mitigated by the inclusion of Hep-MA, due to its ability to crosslink with PEGDA. The other network properties (swelling ratio, mesh size) showed trends that were comparable with molecular weight between crosslinks. Mesh size was additionally investigated to ensure that molecules could diffuse through the gel. Mesh size ranged from ∼50 to 180 Å, which is sufficiently large to allow the diffusion of molecules such as IgG [37].

The finding that the addition of heparin or Hep-MA reduced the flexural stiffness of PEGDA hydrogels was in contrast to the results of Beamish et al., who reported that the incorporation of PEGylated moieties into the gel actually increased the bulk material stiffness [38]. Their finding was surprising, given that it was expected that these additions would decrease the stiffness due to network interruption. Together these works emphasize the importance of investigating the mechanical consequences of adding monoacrylated PEG or other functional sequences (peptides, glycosaminoglycans) to these hydrogels, in addition to the effects of inclusion of these biofunctional moieties on cell phenotype and synthetic ability, which has received far more attention. The effect of bioactive moiety incorporation on hydrogel mechanics is important, and significant enough to merit its own study.

The incorporation of cells into the hydrogels profoundly decreased flexural stiffness, which was most likely caused by their cytoskeletal stiffness and total volume fraction [39]. Because the concentrations of cells typically used in TEHVs are rather high, it is necessary to plan for their effects on hydrogel mechanics [33,34]. Furthermore, the impact of hydrogel swelling on cells has been understudied. Gel swelling could potentially "prestrain" the encapsulated cells, however, for the compositions chosen in this paper this effect of swelling was likely modest, due to both the small volumetric swelling (the resulting strain is substantially lower than what is typically imparted in a mechanical conditioning study) exhibited by the chosen formulations and the immaturity of adhesions between embedded ligands and cells during the swelling period. Gel formulations with very high molecular weights (20 and 35 kDa, unpublished results) demonstrate very high volumetric swelling and in the future it will be necessary to characterize the mechanical forces imparted to the cells by swelling.

The concentration of cells used in this study (22 million cells per ml) is representative of the range of cell concentrations employed in other hydrogel studies [13,32–34]. In the future it will be of interest to evaluate the impact of cell encapsulation on hydrogel mechanics in a concentration-dependent manner. Furthermore, the immunofluorescence showed that as gel stiffness increased the proportion of cells positive for αSMA decreased. The stiffest gel compositions tested (15%, 6 kDa, 100 kPa; 15%, 8 kDa, 150 kPa) showed the lowest proportion of cells expressing αSMA. P4H expression was low throughout all gel compositions, which potentially was due to the short culture duration.

In conclusion, since bending is a major mode of deformation for valves, it is crucial to investigate the flexural properties of materials being considered as TEHV scaffolds. This study is the first to examine flexure of cell-seeded hydrogels. Understanding the bending behavior of cell-seeded, homogeneous hydrogels will permit the creation and characterization of scaffolds with more complicated architectures in the drive to mimic heart valve tissue mechanics more closely. It is important to note that the hydrogels used in this study lacked any cell-degradable motifs. The incorporation of these motifs, however, will be necessary as the scaffold architecture becomes more complex to enable the cells to synthesize matrix and migrate into and remodel the scaffold prior to implantation. Furthermore, this work adds to a recent publication by Beamish et al. [38] in demonstrating that the addition of other crosslinkable groups to PEGDA can radically change the mechanical behavior of the hydrogel. It will be important to consider and account for all of these effects in the design of more complex biomaterials.

Acknowledgements

Appendix A. Supplementary data

Supplementary data associated with this article can be found, in the online version, at doi:10.1016/j.actbio.2011.02.018.

References

[1] Stock UA, Mayer Jr JE. Tissue engineering of cardiac valves on the basis of PGA/PLA co-polymers. J Long Term Effect Med Implants 2001;11:249–60.

[2] Engelmayr Jr GC, Rabkin E, Sutherland FW, Schoen FJ, Mayer Jr JE, Sacks MS. The independent role of cyclic flexure in the early in vitro development of an engineered heart valve tissue. Biomaterials 2005;26:175–87.

[3] Sodian R, Hoerstrup SP, Sperling JS, Martin DP, Daebritz S, Mayer Jr JE, et al. Evaluation of biodegradable, three-dimensional matrices for tissue engineering of heart valves. Asaio J 2000;46:107–10.

[4] Sodian R, Hoerstrup SP, Sperling JS, Daebritz S, Martin DP, Moran AM, et al. Early in vivo experience with tissue-engineered trileaflet heart valves. Circulation 2000;102:III22–9.

[5] Mol A, Bouten CV, Baaijens FP, Zund G, Turina MI, Hoerstrup SP. Review article: tissue engineering of semilunar heart valves: current status and future developments. J Heart Valve Dis 2004;13:272–80.

[6] Mol A, Rutten MC, Driessen NJ, Bouten CV, Zund G, Baaijens FP, et al. Autologous human tissue-engineered heart valves: prospects for systemic application. Circulation 2006;114:I152–8.

[7] Engelmayr Jr GC, Hildebrand DK, Sutherland FW, Mayer Jr JE, Sacks MS. A novel bioreactor for the dynamic flexural stimulation of tissue engineered heart valve biomaterials. Biomaterials 2003;24:2523–32.

[8] Nemir S, Hayenga HN, West JL. PEGDA hydrogels with patterned elasticity: novel tools for the study of cell response to substrate rigidity. Biotechnol Bioeng 2010;105:636–44.

[9] Hahn MS, Miller JS, West JL. Three-dimensional biochemical and biomechanical patterning of hydrogels for guiding cell behavior. Adv Mater 2006;18:2679–84.

[10] Lee SH, Moon JJ, Miller JS, West JL. Poly(ethylene glycol) hydrogels conjugated with a collagenase-sensitive fluorogenic substrate to visualize collagenase activity during three-dimensional cell migration. Biomaterials 2007;28:3163–70.

[11] Hoerstrup SP, Sodian R, Daebritz S, Wang J, Bacha EA, Martin DP, et al. Functional living trileaflet heart valves grown in vitro. Circulation 2000;102:III44–9.

[12] Burg KJ, Holder Jr WD, Culberson CR, Beiler RJ, Greene KG, Loebsack AB, et al. Comparative study of seeding methods for three-dimensional polymeric scaffolds. J Biomed Mater Res 2000;51:642–9.

[13] Mol A, van Lieshout MI, Dam-de Veen CG, Neuenschwander S, Hoerstrup SP, Baaijens FP, et al. Fibrin as a cell carrier in cardiovascular tissue engineering applications. Biomaterials 2005;26:3113–21.

[14] Benton JA, Kern HB, Anseth KS. Substrate properties influence calcification in valvular interstitial cell culture. J Heart Valve Dis 2008;17:689–99.

[15] Cushing MC, Liao JT, Jaeggli MP, Anseth KS. Material-based regulation of the myofibroblast phenotype. Biomaterials 2007;28:3378–87.

[16] Hahn MS, McHale MK, Wang E, Schmedlen RH, West JL. Physiologic pulsatile flow bioreactor conditioning of poly(ethylene glycol)-based tissue engineered vascular grafts. Ann Biomed Eng 2007;35:190–200.

[17] Leslie-Barbick JE, Moon JJ, West JL. Covalently-immobilized vascular endothelial growth factor promotes endothelial cell tubulogenesis in poly(ethylene glycol) diacrylate hydrogels. J Biomater Sci 2009;20:1763–79.

[18] Weber LM, Anseth KS. Hydrogel encapsulation environments functionalized with extracellular matrix interactions increase islet insulin secretion. Matrix Biol 2008;27:667–73.

[19] Peyton SR, Raub CB, Keschrumrus VP, Putnam AJ. The use of poly(ethylene glycol) hydrogels to investigate the impact of ECM chemistry and mechanics on smooth muscle cells. Biomaterials 2006;27:4881–93.

[20] Benoit DS, Durney AR, Anseth KS. The effect of heparin-functionalized PEG hydrogels on three-dimensional human mesenchymal stem cell osteogenic differentiation. Biomaterials 2007;28:66–77.

[21] Temenoff JS, Athanasiou KA, LeBaron RG, Mikos AG. Effect of poly(ethylene glycol) molecular weight on tensile and swelling properties of oligo(poly(ethylene glycol) fumarate) hydrogels for cartilage tissue engineering. J Biomed Mater Res 2002;59:429–37.

[22] Cuchiara MP, Allen AC, Chen TM, Miller JS, West JL. Multilayer microfluidic PEGDA hydrogels. Biomaterials 2010;31:5491–7.

[23] Cloyd JM, Malhotra NR, Weng L, Chen W, Mauck RL, Elliott DM. Material properties in unconfined compression of human nucleus pulposus, injectable hyaluronic acid-based hydrogels and tissue engineering scaffolds. Eur Spine J 2007;16:1892–8.

[24] Stephens EH, Chu CK, Grande-Allen KJ. Valve proteoglycan content and glycosaminoglycan fine structure are unique to microstructure, mechanical load and age: relevance to an age-specific tissue-engineered heart valve. Acta Biomater 2008;4:1148–60.

[25] Mirnajafi A, Raymer J, Scott MJ, Sacks MS. The effects of collagen fiber orientation on the flexural properties of pericardial heterograft biomaterials. Biomaterials 2005;26:795–804.

[26] Bryant SJ, Chowdhury TT, Lee DA, Bader DL, Anseth KS. Crosslinking density influences chondrocyte metabolism in dynamically loaded photocrosslinked poly(ethylene glycol) hydrogels. Ann Biomed Eng 2004;32:407–17.

[27] Almany L, Seliktar D. Biosynthetic hydrogel scaffolds made from fibrinogen and polyethylene glycol for 3D cell cultures. Biomaterials 2005;26:2467–77.

[28] Smeds KA, Grinstaff MW. Photocrosslinkable polysaccharides for in situ hydrogel formation (vol. 54, p. 115, 2000). J Biomed Mat Res 2001;55:254–5.

[29] Gloeckner DC, Billiar KL, Sacks MS. Effects of mechanical fatigue on the bending properties of the porcine bioprosthetic heart valve. Asaio J 1999;45:59–63.

[30] Messier Jr RH, Bass BL, Aly HM, Jones JL, Domkowski PW, Wallace RB, et al. Dual structural and functional phenotypes of the porcine aortic valve interstitial population: characteristics of the leaflet myofibroblast. J Surg Res 1994;57:1–21.

[31] Cruise GM, Scharp DS, Hubbell JA. Characterization of permeability and network structure of interfacially photopolymerized poly(ethylene glycol) diacrylate hydrogels. Biomaterials 1998;19:1287–94.

[32] Benton JA, Deforest CA, Vivekanandan V, Anseth KS. Photocrosslinking of gelatin macromers to synthesize porous hydrogels that promote valvular interstitial cell function. Tissue Eng Part A 2009;15:3221–30.

[33] Masters KS, Shah DN, Leinwand LA, Anseth KS. Crosslinked hyaluronan scaffolds as a biologically active carrier for valvular interstitial cells. Biomaterials 2005;26:2517–25.

[34] Benton JA, Fairbanks BD, Anseth KS. Characterization of valvular interstitial cell function in three dimensional matrix metalloproteinase degradable PEG hydrogels. Biomaterials 2009;30:6593–603.

[35] Thubrikar MJ. The aortic valve. Boca Raton, FL: CRC Press; 1990.

[36] Merryman WD, Huang HY, Schoen FJ, Sacks MS. The effects of cellular contraction on aortic valve leaflet flexural stiffness. J Biomech 2006;39:88–96.

[37] Jossang T, Feder J, Rosenqvist E. Photon correlation spectroscopy of human IgG. J Protein Chem 1988;7:165–71.

[38] Beamish JA, Zhu J, Kottke-Marchant K, Marchant RE. The effects of monoacrylated poly(ethylene glycol) on the properties of poly(ethylene glycol) diacrylate hydrogels used for tissue engineering. J Biomed Mater Res A 2010;92:441–50.

[39] Jones RM. Mechanics of composite materials. New York: Hemisphere Publishing Corp.; 1975.